DALTON

Crystal structures and non-linear optical properties of cluster compounds $[MAu_2S_4(AsPh_3)_2]$ (M = Mo or W)†

He-gen Zheng,[a] Wei Ji,[b] Michael L. K. Low,[b] Genta Sakane,[c] Takashi Shibahara[c] and Xin-quan Xin*,[a]

[a] *State Key Laboratory of Coordination Chemistry, Coordination Chemistry Institute, Nanjing University, Nanjing, 210093, People's Republic of China*
[b] *Department of Physics, National University of Singapore, Singapore 119260, Republic of Singapore*
[c] *Department of Chemistry, Okayama University of Science, Okayama 700, Japan*

The compounds $[MAu_2S_4(AsPh_3)_2]$ (M = Mo **1** or W **2**) were synthesized by reactions of $[NEt_4]_2[MS_4]$ (M = Mo or W), $HAuCl_4·4H_2O$ and $AsPh_3$ in CH_2Cl_2 solution. X-Ray crystallographic structure determinations show that the co-ordination of Mo(W) is slightly distorted from tetrahedral and those of the Au are distorted from trigonal planar. High non-linear susceptibilities of these gold-containing clusters were also observed for the first time. Z-Scan data measured with 532 nm nanosecond laser pulses showed that effective third-order non-linearities $\alpha_2 = 7.9 \times 10^{-5}$ and 13×10^{-5} dm³ cm W^{-1} mol^{-1} and $n_2 = -8.0 \times 10^{-10}$ and 19×10^{-10} dm³ cm^2 W^{-1} mol^{-1}, respectively, for a 0.64 mmol dm^{-3} solution of compound **1** and a 0.54 mmol dm^{-3} solution of **2**.

The Mo(W)–Cu(Ag)–S cluster compounds have been studied extensively in the past two decades, because of their relevance to biological systems and catalytic processes.[1,2] Recently, we have noticed that they also exhibit very interesting non-linear optical (NLO) properties. For example, strong NLO behaviour has been reported in nest-shaped clusters $[NBu^n_4]_2[MoCu_3OS_3(NCS)_3]$ and $[NBu^n_4]_2[MoCu_3OS_3BrCl_2]$, a supracage-shaped cluster $[NBu^n_4]_4[Mo_8Cu_{12}O_8S_{24}]$, and a twin nest-shaped cluster $[NEt_4]_4[Mo_2Cu_6OS_6Br_2I_4]$.[3–5] Butterfly-shaped clusters $[MCu_2OS_3(PPh_3)_n]$ (M = Mo or W, n = 3 or 4) and a half-open cage-shaped cluster $[NEt_4]_3[W(CuBr)_3OS_3(\mu\text{-Br})]·2H_2O$ exhibit large NLO refraction.[6,7] Cubane-like clusters $[NBu^n_4]_3[MM'_3S_4Br(X)]$ (M = Mo or W, M′ = Cu or Ag, X = Cl or I) possess strong NLO absorption.[8] A very large optical limiting effect has been observed in a hexagonal prism-shaped cluster $[Mo_2Ag_4S_8(PPh_3)_4]$, which is about ten times larger than that observed in C_{60}.[9] In order to explore this field further, we have synthesized a series of new Mo(W)–Au–S cluster compounds. In this article we report the synthesis, characterization and NLO properties of gold-containing compounds with a linear structure, $[MoAu_2S_4(AsPh_3)_2]$ **1** and $[WAu_2S_4(AsPh_3)_2]$ **2**.

Experimental

Materials

Compounds $[NEt_4]_2[MoS_4]$ and $[NEt_4]_2[WS_4]$ were prepared according to a literature method.[10] Other chemicals were of AR grade and used without further purification.

Preparations

$[MoAu_2S_4(AsPh_3)_2]$ 1. Triphenylarsine (120.3 mg, 0.3931 mmol) dissolved in CH_2Cl_2 (5 cm^3) was slowly added to $HAuCl_4·4H_2O$ (81 mg, 0.1966 mmol) in absolute ethanol (5 cm^3). The light yellow solution was stirred for 2 h and refrigerated at 5 °C overnight. The resulting colourless crystals were dissolved in CH_2Cl_2 (15 cm^3) and $[NEt_4]_2[MoS_4]$ (47.64 mg, 0.0983 mmol) was added. After stirring for 1 h the red-black solution was filtered and Pr^iOH (10 cm^3) was added dropwise to the top of the solution. The red crystals were obtained several days later (Found: C, 35.15; H, 2.4. Calc. for $C_{36}H_{30}As_2Au_2MoS_4$: C, 35.15; H, 2.45%). IR (KBr pellet, cm^{-1}): C–H in $AsPh_3$, 734.1vs, 689.3vs; Au–P, 614.6w; Mo–S_b, 453.4vs.

$[WAu_2S_4(AsPh_3)_2]$ 2. The synthetic method was similar to that used for compound **1**, $[NEt_4]_2[WS_4]$ being used instead of $[NEt_4]_2[MoS_4]$. Yellow crystals were obtained (Found: C, 32.75; H, 2.32. Calc. for $C_{36}H_{30}As_2Au_2S_4W$: C, 32.8; H, 2.3%). IR (KBr pellet, cm^{-1}): C–H in $AsPh_3$, 737.5vs, 688.3vs; Au–P, 519.5w; W–S_b, 477.3vs, 442.2vs, 407.0w.

X-Ray crystallography

A red crystal of compound **1** was mounted in a glass capillary. All measurements were made on a Rigaku AFC6S diffractometer with graphite-monochromated Mo-Kα radiation (λ = 0.7107 Å). The lattice parameters shown in Table 1 were refined using 21 reflections in the range $9.4 < \theta < 12.7°$. The data collection with ω–2θ scans between 3 and 25° resulted in 6949 intensity values, 4591 with $I > 1.50\sigma(I)$ being used for the structure determination. The structure was solved by heavy-atom Patterson methods[11] and expanded using Fourier techniques.[12] The non-hydrogen atoms were refined anisotropically. Hydrogen atoms were included but not refined. The final cycle of full-matrix least-squares refinement converged with unweighted and weighted agreement factors $R = 0.0299$ and $R' = 0.0387$.

For compound **2**, an orange crystal was mounted in a glass capillary for X-ray data collection. All measurements were made on a Mac Science MXC-18 diffractometer. The lattice parameters (Table 1) were refined using 39 reflections in the range $10.0 < \theta < 15.0°$. The data collection with ω–2θ scans between 3 and 30° resulted in 11 491 intensity values, 7676 with $I > 1.50\sigma(I)$ being used for the structure determination. The structure was solved by direct methods[13] and expanded using Fourier techniques. The refinement was based on F. An empirical absorption correction using the program DIFABS[14] was applied. The data were corrected for Lorentz-polarization effects, and the final $R = 0.0638$ and $R' = 0.0859$. The function minimised was $\Sigma w(|F_o| - |F_c|)^2$, where $w = 1/\sigma^2(F_o)$.

All calculations were performed using the TEXSAN[15] crys-

† *Non-SI unit employed*: eV ≈ 1.60×10^{-19} J.

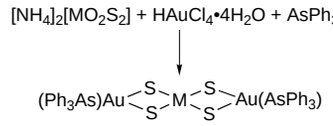

Scheme 1

$$3[MO_2S_2]^{2-} \rightleftharpoons 2[MOS_3]^{2-} + [MO_4]^{2-}$$

$$4[MOS_3]^{2-} \rightleftharpoons 3[MS_4]^{2-} + [MO_4]^{2-}$$

Scheme 2

tallographic software package. Selected bond distances and angles are given in Tables 2 and 3.

Atomic coordinates, thermal parameters, and bond lengths and angles have been deposited at the Cambridge Crystallographic Data Centre (CCDC). See Instructions for Authors, *J. Chem. Soc., Dalton Trans.*, 1997, Issue 1. Any request to the CCDC for this material should quote the full literature citation and the reference number 186/499.

Physical measurements

Infrared spectra were recorded on a Fourier Nicolet FT-10SX spectrophotometer with pressed KBr pellets, electronic spectra with a Hitachi U-3410 spectrophotometer. Carbon and hydrogen analyses were performed on a PE-240C elemental analyser.

Non-linear optical measurements

The NLO properties of compounds **1** and **2** dissolved in CH_2Cl_2 were determined by using a standard Z-scan set up with a Q-switched, frequency-doubled Nd:YAG laser. The pulse repetition rate was 10 Hz. The details of the set-up can be found elsewhere.[16] The solutions were contained in 1 mm thick quartz cells with concentrations of 6.4×10^{-4} and 5.4×10^{-4} mol dm^{-3} for compounds **1** and **2**, respectively.

Results and Discussion

Synthesis

The compounds were synthesized from $[NEt_4]_2[MS_4]$ (M = Mo or W), $HAuCl_4 \cdot 4H_2O$ and $AsPh_3$ in CH_2Cl_2 solution. When $[NEt_4]_2[MO_2S_2]$ was used instead of $[NEt_4]_2[MS_4]$, the same compounds were obtained, as in Scheme 1. The transformation from $[MO_2S_2]^{2-}$ to $[MS_4]^{2-}$ may take place as in Scheme 2. Therefore, the $[MS_4]^{2-}$ anion reacts with $[Au(AsPh_3)]^+$ to give the products. However, an interesting fact is that $[MoOS_3(AuPPh_3)\{Au(PPh_3)_2\}]$ was synthesized in poor yield by reaction of $Cs_2[MoOS_3]$ and $[Au(PPh_3)Cl]$.[17]

Structures of $[MAu_2S_4(AsPh_3)_2]$ (M = Mo 1 or W 2)

Figs. 1 and 2 show the crystal structures of compounds **1** and **2**, Figs. 3 and 4 the packings of the clusters in the solid state. The skeletons, consisting of one M, four μ-S and two Au atoms, show linear structures with crystallographic C_{2v} symmetry. The Au–Mo–Au and Au–W–Au angles are 178.51(3) and 178.27(2)°, respectively. The M (Mo or W) atom has essentially tetrahedral co-ordination and MS_4^{2-} acts as a tetradentate ligand co-ordinating to two Au atoms through its four μ-S atoms. Each Au atom is co-ordinated by two μ-S atoms and one $AsPh_3$ ligand, forming a planar trigonal geometry.

The $MS^1S^2Au^1$ and $MS^3S^4Au^2$ (M = Mo or W) cores in compounds **1** and **2** are planar to within 0.0056 (0.0083) and 0.0125 (0.0136) Å, respectively. Their dihedral angle is 89.65 (89.73)°, which means that they are essentially perpendicular to each other.

There are two types of structures in related linear compounds as depicted in Scheme 3; the main bond lengths are listed in Table 4, which reveals several structural trends. First, in all linear-shaped compounds $MS_2M'_2$ (M = Mo or W; M′ = Cu, Ag or Au), each Au atom in compounds **1**, **2**, **6** and **10** is in a trigonal-planar co-ordination; one Cu(Ag) atom in **3**–**5** and **7**–**9** is tetrahedrally co-ordinated and the other is trigonally co-ordinated. However, the co-ordination modes of two Au atoms in the nest-shaped compound $[MoOS_3(AuPPh_3)\{Au(PPh_3)_2\}]$ are the same as those observed in linear-shaped Mo(W)–Cu(Ag)–S cluster compounds. Secondly, the M–S bond lengths of four gold-containing linear compounds are similar to each other. Owing to the influences of the ligands, the Mo–Au, W–Au and Au–S bond lengths are different. The Au–As bond lengths are, of course, longer than corresponding Au–P distances. The explanation for this fact is that the covalent radius (1.21 Å) of As is longer than that (1.10 Å) of P. Thirdly, the Au–P bond length [2.272(2) Å for **6**] trigonally co-ordinated in Mo–M′–L (M′ = Cu, Ag or Au) compounds **3**, **4**,

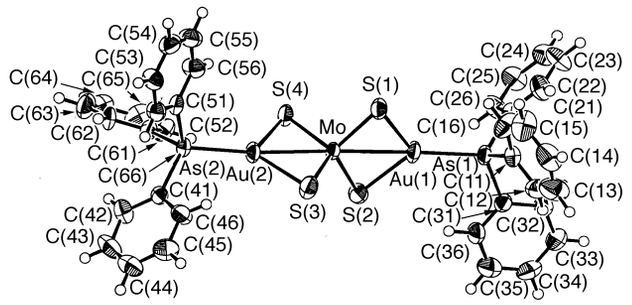

Fig. 1 Crystal structure of $[MoAu_2S_4(AsPh_3)_2]$

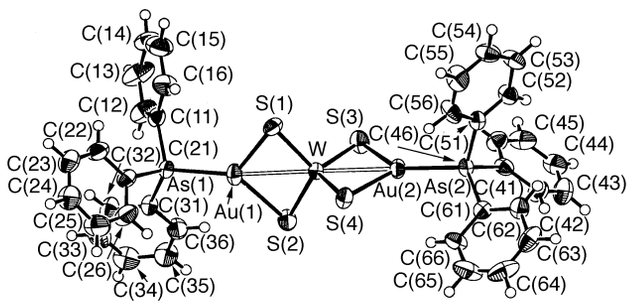

Fig. 2 Crystal structure of $[WAu_2S_4(AsPh_3)_2]$

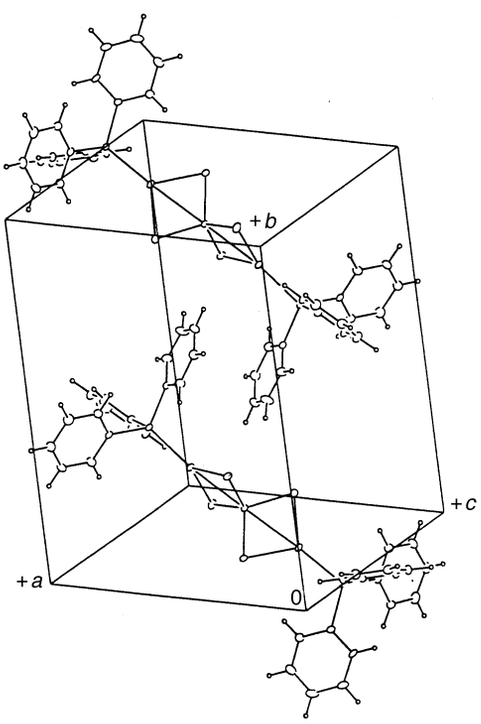

Fig. 3 Packing of $[MoAu_2S_4(AsPh_3)_2]$ in the solid state

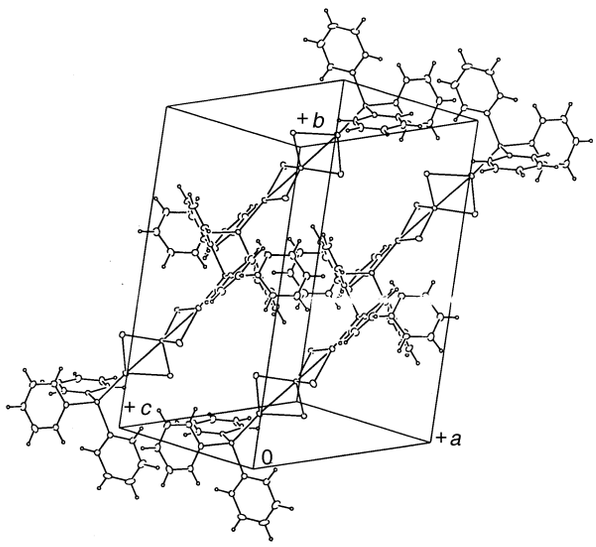

Fig. 4 Packing of $[WAu_2S_4(AsPh_3)_2]$ in the solid state

Table 1 Crystal data and experimental parameters for complexes **1** and **2***

	1	**2**
Formula	$C_{36}H_{30}As_2Au_2MoS_4$	$C_{36}H_{30}As_2Au_2S_4W$
M	1230.59	1318.50
Crystal size/mm	0.41 × 0.20 × 0.16	0.50 × 0.41 × 0.30
a/Å	9.580(4)	9.572(2)
b/Å	10.753(4)	10.803(2)
c/Å	19.838(8)	19.816(4)
α/°	88.12(4)	88.15(1)
β/°	80.20(4)	80.30(2)
γ/°	67.39(3)	67.52(2)
U/Å^3	1857(1)	1865.2(7)
T/K	290.2	295.2
D_c/g cm^{-3}	2.200	2.348
F(000)	1152.00	1216.00
μ(Mo-Kα)/cm^{-1}	102.55	129.64
$2\theta_{max}$/°	50.0	60.0
Scan speed/° min^{-1}	2.0	8.0
No. observations [$I > 1.5\sigma(I)$]	4591	7676
R	0.0299	0.0638
R′	0.0387	0.0859
Goodness of fit indicator	1.108	0.935
Maximum, minimum peaks in final difference map/e Å^{-3}	0.96, −0.71	6.85, −5.29

* Details in common: triclinic, space group $P\bar{1}$; $Z = 2$; 407 variables; maximum shift in final cycle 0.00.

and **6** is between the Cu–P [2.210(5) Å] and Ag–P distances [2.380(4) Å], though atom covalent radii vary as Au > Ag > Cu, showing that the Au–P bond is stronger than the Cu–P and Ag–P. The same trend is observed in W–M′–S compounds **7**, **8** and **10**. Fourthly, M′–P, M′–S and M–M′ bond lengths in tetrahedral co-ordination are longer than those in trigonal co-ordination in compounds **3**–**5** and **7**–**9**. However, the opposite trend is found in M–S bond distances.

NLO properties of $[MAu_2S_4(AsPh_3)_2]$ (M = Mo 1 or W 2)

The similarity in the structures of the two compounds should lead to similar UV/VIS spectra, which is confirmed by Fig. 5. The red shift in the spectrum of compound **1** is expected since it contains one Mo atom instead of one W atom. The first absorption peaks are located at 500 (2.48) and 410 nm (3.02 eV) for compounds **1** and **2**, respectively. Their Z-scan results are shown in Fig. 6, where the filled and open circles were measured

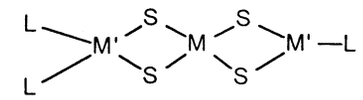

M = Mo, W
M′ = Cu, Ag
L = PPh_3, CN

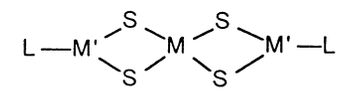

M = Mo, W
M′ = Au
L = PPh_3, $AsPh_3$, Ph_2PCH_3

Scheme 3

Table 2 Selected bond distances (Å) and angles (°) for compound **1**

Au(1)–Mo	2.7837(7)	Au(1)–As(1)	2.3745(8)
Au(1)–S(1)	2.395(2)	Au(1)–S(2)	2.392(2)
Au(2)–Mo	2.7690(7)	Au(2)–As(2)	2.3715(8)
Au(2)–S(3)	2.378(2)	Au(2)–S(4)	2.396(2)
Mo–S(1)	2.216(2)	Mo–S(2)	2.213(2)
Mo–S(3)	2.214(2)	Mo–S(4)	2.213(2)
Mo–Au(1)–As(1)	172.74(3)	Mo–Au(1)–S(1)	49.97(5)
Mo–Au(1)–S(2)	49.93(5)	As(1)–Au(1)–S(1)	126.55(6)
As(1)–Au(1)–S(2)	133.10(6)	S(1)–Au(1)–S(2)	99.89(7)
Mo–Au(2)–As(2)	174.86(3)	Mo–Au(2)–S(3)	50.26(6)
Mo–Au(2)–S(4)	50.10(5)	As(2)–Au(2)–S(3)	134.31(6)
As(2)–Au(2)–S(4)	125.23(6)	S(3)–Au(2)–S(4)	100.36(8)
Au(1)–Mo–Au(2)	178.51(3)	Au(1)–Mo–S(1)	55.86(6)
Au(1)–Mo–S(2)	55.80(6)	Au(1)–Mo–S(3)	123.44(7)
Au(1)–Mo–S(4)	124.70(6)	Au(2)–Mo–S(1)	125.34(6)
Au(2)–Mo–S(2)	123.01(7)	Au(2)–Mo–S(3)	55.68(6)
Au(2)–Mo–S(4)	56.18(6)	S(1)–Mo–S(2)	111.65(9)
S(1)–Mo–S(3)	109.07(10)	S(1)–Mo–S(4)	108.24(9)
S(2)–Mo–S(3)	108.13(10)	S(2)–Mo–S(4)	107.92(10)
S(3)–Mo–S(4)	111.86(9)	Au(1)–S(1)–Mo	74.15(7)
Au(1)–S(2)–Mo	74.28(7)	Au(2)–S(3)–Mo	74.06(7)
Au(2)–S(4)–Mo	73.72(7)		

Table 3 Selected bond distances (Å) and angles (°) for compound **2**

Au(1)–W	2.8103(4)	Au(1)–As(1)	2.3733(9)
Au(1)–S(1)	2.427(3)	Au(1)–S(2)	2.406(3)
Au(2)–W	2.7951(4)	Au(2)–As(2)	2.3698(9)
Au(2)–S(3)	2.400(3)	Au(2)–S(4)	2.418(3)
W–S(1)	2.213(2)	W–S(2)	2.217(2)
W–S(3)	2.213(3)	W–S(4)	2.218(2)
W–Au(1)–As(1)	172.38(3)	W–Au(1)–S(1)	49.32(6)
W–Au(1)–S(2)	49.55(6)	As(1)–Au(1)–S(1)	126.65(6)
As(1)–Au(1)–S(1)	134.02(6)	S(1)–Au(1)–S(2)	98.86(8)
W–Au(2)–As(2)	174.63(3)	W–Au(2)–S(3)	49.72(6)
W–Au(2)–S(4)	49.71(6)	As(2)–Au(2)–S(3)	135.12(7)
As(2)–Au(2)–S(4)	125.34(6)	S(3)–Au(2)–S(4)	99.42(9)
Au(1)–W–Au(2)	178.27(2)	Au(1)–W–S(1)	56.28(7)
Au(1)–W–S(2)	55.70(7)	Au(1)–W–S(3)	123.15(7)
Au(1)–W–S(4)	124.77(7)	Au(2)–W–S(1)	125.11(7)
Au(2)–W–S(2)	122.93(7)	Au(2)–W–S(3)	55.81(7)
Au(2)–W–S(4)	56.27(6)	S(1)–W–S(2)	111.96(10)
S(1)–W–S(3)	108.6(1)	S(1)–W–S(4)	108.14(10)
S(2)–W–S(3)	108.3(1)	S(2)–W–S(4)	107.9(1)
S(3)–W–S(4)	112.08(10)	Au(1)–S(1)–W	74.40(7)
Au(1)–S(2)–W	74.75(7)	Au(2)–S(3)–W	74.47(8)
Au(2)–S(4)–W	74.02(7)		

with and without the aperture, respectively. To obtain the NLO parameters we employed a Z-scan theory which considers effective non-linearities of third-order nature only: $\alpha = \alpha_0 + \alpha_2 I$

Table 4 Comparison of main bond distances (Å)[a]

	Compound	M–S[b]	M–M′[b]	M′–S[b]	M′–L	Ref.
1	$[MoAu_2S_4(AsPh_3)_2]$	2.214(2)	2.7764(7)	2.390(2)	2.373(8)	This work
3	$[MoCu_2S_4(PPh_3)_3]\cdot 0.8CH_2Cl_2$	2.218(5)	2.642(3)	2.220(5)	2.210(5)	18
		2.198(5)*	2.775(2)*	2.313(5)*	2.303(5)*	
4	$[MoAg_2S_4(PPh_3)_3]\cdot 0.8CH_2Cl_2$	2.215(5)	2.860(2)	2.459(5)	2.380(4)	19
		2.195(5)*	3.030(2)*	2.572(5)*	2.471(4)*	
5	$[NEt_4][MoAg(CuCN)S_4(PPh_3)_2]$	2.202(6)	2.622(3)	2.209(7)	1.87(2)	20
		2.189(5)*	3.075(2)*	2.584(5)*	2.484(5)*	
6	$[MoAu_2S_4(PPh_3)_2]$	2.214(2)	2.810(1)	2.405(2)	2.272(2)	17
2	$[WAu_2S_4(AsPh_3)_2]$	2.215(2)	2.8027(4)	2.413(3)	2.372(9)	This work
7	$[WCu_2S_4(PPh_3)_3]\cdot 0.8CH_2Cl_2$	2.224(8)	2.670(3)	2.232(9)	2.209(8)	19
		2.204(3)*	2.809(3)*	2.333(3)*	2.307(8)*	
8	$[WAg_2S_4(PPh_3)_3]\cdot 0.8CH_2Cl_2$	2.219(1)	2.886(2)	2.476(6)	3.362(5)	19
		2.195(5)*	3.056(2)*	2.579(5)*	2.460(1)*	
9	$[NEt_4][WAg(CuCN)S_4(PPh_3)_2]$	2.202(5)	2.638(3)	2.219(6)	1.82(2)	21
		2.189(5)*	3.099(2)*	2.596(5)*	2.479(5)*	
10	$[WAu_2S_4(PMePh_2)_2]$	2.219(3)	2.841(1)	2.429(3)	2.268(3)	22
11	$[MoOS_3(AuPPh_3)\{Au(PPh_3)_2\}]$	2.261(2)	2.838(1)	2.419(2)	2.277(2)	17
		2.241(2)*	3.133(1)*	2.644(2)*	2.325(2)*	

[a] M = Mo or W; M′ = Cu, Ag or Au. [b] Average values. * The starred bond lengths are those when the Cu or Ag has tetrahedral co-ordination and the S or P atom is bonded to the Cu or Ag.

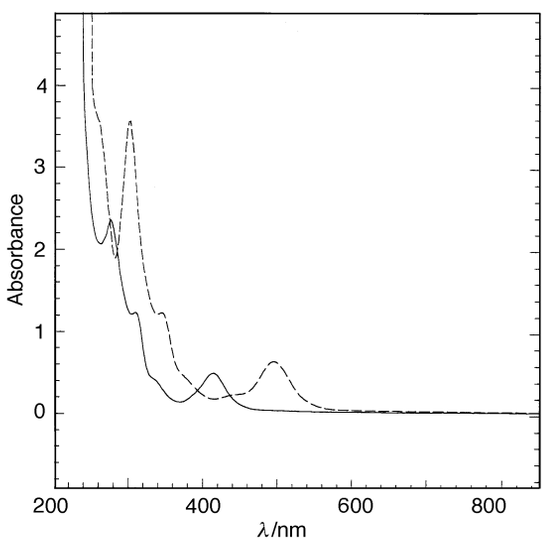

Fig. 5 Electronic spectra of $[MoAu_2S_4(AsPh_3)_2]$ (9.6×10^{-5} mol dm^{-3}) (– – –) and $[WAu_2S_4(AsPh_3)_2]$ (4.2×10^{-4} mol dm^{-3}) (——) in CH_2Cl_2. Optical path 1 cm

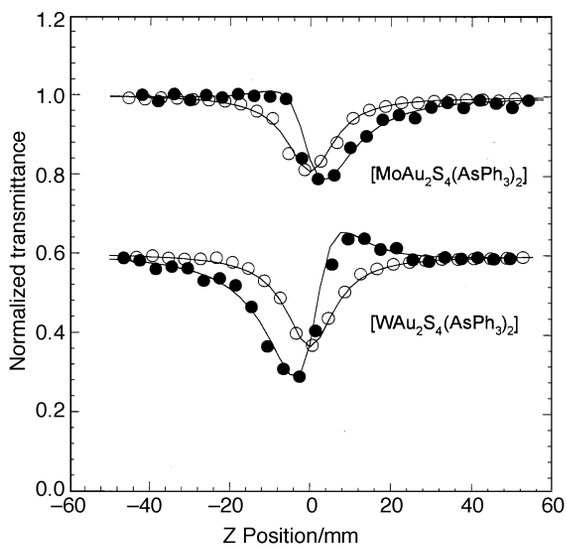

Fig. 6 Z Scans of $[MoAu_2S_4(AsPh_3)_2]$ (6.4×10^{-4} mol dm^{-3}) and $[WAu_2S_4(AsPh_3)_2]$ (5.4×10^{-4} mol dm^{-3}) with 532 nm, 7 ns laser pulses. Optical path 1 mm. Incident energy of pulses 20 mJ. Transmittance of the aperture 0.34. The experimental data were measured with (●) and without (○) the aperture, respectively. The solid curves represent fits based on Z-scan theory. The Z scans of $[WAu_2S_4(AsPh_3)_2]$ have been vertically displaced by 0.4 for clarity

and $n = n_0 + n_2 I$, where α, α_0 and α_2 are the total, linear and non-linear absorption coefficients, n, n_0 and n_2 the total, linear and non-linear refractive indices and I is the light irradiance. The details of the theory can be found elsewhere.[16] The good fits between the theory and the Z-scan data suggest that the observed non-linearities can be expressed effectively by third-order susceptibilities. The values of α_2 and n_2 extracted from the best fits are listed in Table 5. The modulus of the third-order molecular susceptibility was calculated from equation (1) where

$$|\gamma| = \frac{1}{NF^4}\sqrt{\left(\frac{9 \times 10^8 \varepsilon_0 n_0^2 c^2 \alpha_2}{4\pi\omega}\right)^2 + \left(\frac{c n_0^2 n_2}{80\pi^2}\right)^2} \qquad (1)$$

ε_0 and c are the permittivity and the speed of light in a vacuum, respectively, ω is the angular frequency of the light, N the compound concentration, and F^4 the local Lorentz field. In this expression all the units are SI except that N is in cm^{-3} and $|\gamma|$ is in esu. Assuming that $F^4 = 3$, we calculate that $|\gamma| = 3.0 \times 10^{-29}$ and 6.5×10^{-29} esu (esu = 7.162×10^{13} m^5 v^{-2}) for compounds **1** and **2**, respectively. Note that such a large γ value is measured in the transparent region for compound **2**, and is several orders of magnitude greater than those in well known NLO materials in the transparent part of their spectra (for example: 5.6×10^{-35}–8.6×10^{-34} esu for Group 10 metal alkynyl polymers at 1064 nm,[23,24] 1×10^{-32}–1×10^{-31} esu for metallophthalocyanines at 1064 nm[25] and 7.5×10^{-34} esu for C_{60} at 1910 nm).[26] It is also interesting to compare these two new compounds with clusters that we have previously reported. Table 5 shows that compound **2** compares favourably with all the clusters in terms of figures of merit, α_2/α_0 and n_2/α_0.

It should be emphasized that the Z scans reported here could not reveal the origins of the observed non-linearities. Excited-state absorption and non-linear scattering are possible for the measured absorptive non-linearity. The change in the sign of the measured refractive non-linearity may give a hint as to the cause of the non-linear refraction. The signs of refractive non-linearities for all the clusters, listed in Table 5, show that n_2 alters from positive to negative as the ratio of the photon energy ($h\omega$) to that of the first absorption peak ($h\omega_0$) approaches 1:1. The turning point is located at around $h\omega/h\omega_0 \approx 0.8:1$, which is consistent with a recently developed theory on bound-electronic effects.[27]

Table 5 NLO Parameters for clusters measured at photon energy $h\omega = 2.33$ eV

Cluster	$h\omega_0$/eV	$h\omega/h\omega_0$	10^{-3} α_0/dm^3 cm^{-1} mol^{-1}	10^5 α_2/dm^3 cm W^{-1} mol^{-1}	10^{10} n_2/dm^3 cm^2 W^{-1} mol^{-1}	10^8 $\alpha_2\alpha_0^{-1}$/cm^2 W^{-1}	10^3 $\lvert n_2/\alpha_0\rvert$/cm^3 W^{-1}
$[WCu_2OS_3(PPh_3)_4]$ [a]	4.85	0.48	2.5	≈0	6.7	≈0	2.7
$[MoCu_2OS_3(PPh_3)_3]$ [a]	4.80	0.49	15	35	68	2.3	4.5
$[Mo_2Ag_4S_8(PPh_3)_4]$ [b]	4.75	0.49	6.4	100	120	16	19
$[NEt_4]_3[WOS_3(CuBr)_3(\mu\text{-}Br)]\cdot 2H_2O$ [c]	3.55	0.66	5.3	6.6	12	1.2	2.3
$[WAu_2S_4(AsPh_3)_2]$ [d]	3.02	0.77	0.44	13	19	29	42
$[NBu^n_4]_2[MoCu_3OS_3(NCS)_3]$ [e]	2.50	0.93	1.2	0.18	−1.7	0.15	1.4
$[MoAu_2S_4(AsPh_3)_2]$ [d]	2.48	0.94	4.5	7.9	−8.0	1.8	1.8
$[NBu^n_4]_4[Mo_8Cu_{12}O_8S_{24}]$ [f]	2.43	0.96	7.5	28	−23	3.7	3.1

[a] Ref. 5. [b] Ref. 9. [c] Ref. 7. [d] This work. [e] Ref. 3. [f] Ref. 4.

References

1 R. H. Holm, *Chem. Soc. Rev.*, 1981, **10**, 455.
2 E. D. Simhon, N. C. Baenziger, M. Kanatzidis, M. Draganjac and D. Coucouvanis, *J. Am. Chem. Soc.*, 1981, **103**, 1218.
3 S. Shi, W. Ji, W. Xie, T. C. Chong, H. C. Zeng, J. P. Lang and X. Q. Xin, *Mater. Chem. Phys.*, 1995, **39,** 298; W. Ji, P. Ge, W. Xie, S. H. Tang and S. Shi, *J. Lumin.*, 1996, **66/67**, 115; H. W. Hou, X. R. Ye, X. Q. Xin, J. Liu, M. Q. Chen and S. Shi, *Chem. Mater.*, 1995, **7**, 472.
4 S. Shi, W. Ji and X. Q. Xin, *J. Phys. Chem.*, 1995, **99**, 894; W. Ji, W. Xie, S. H. Tang and S. Shi, *Mater. Chem. Phys.*, 1995, **43**, 45.
5 H. W. Hou, X. Q. Xin, J. Liu, M. Q. Chen and S. Shi, *J. Chem. Soc., Dalton Trans.*, 1994, 3211.
6 Z. R. Chen, H. W. Hou, X. Q. Xin, B. Yu and S. Shi, *J. Chem. Phys.*, 1995, **99**, 8717.
7 S. Shi, H. W. Hou and X. Q. Xin, *J. Phys. Chem.*, 1995, **99**, 4050.
8 S. Shi, W. Ji, S. H.Tang, J. P. Lang and X. Q. Xin, *J. Am. Chem. Soc.*, 1994, **116**, 3615; S. Shi, W. Ji, J. P. Lang and X. Q. Xin, *J. Phys. Chem.*, 1994, **98**, 3570; W. Ji, H. J. Du, S. H. Tang and S. Shi, *J. Opt. Soc. Am. B*, 1996, **12**, 876.
9 W. Ji, S. Shi, H. J. Du, P. Ge, S. W. Tang and X. Q. Xin, *J. Phys. Chem.*, 1995, **99**, 17 297.
10 J. W. McDonald, G. D. Friesen, L. D. Rosenhein and W. E. Newton, *Inorg. Chim. Acta*, 1983, **72**, 205.
11 PATTY, P. T. Beurskens, G. Admiraal, G. Beurskens, W. P. Bosman, S. Garcia-Granda, R. O. Gould, J. M. M. Smits and C. Smykalla, The DIRDIF program system, Technical Report of the Crystallography Laboratory, University of Nijmegen, 1992.
12 P. T. Beurskens, G. Admiraal, G. Beurskens, W. P. Bosman, R. Gelder, R. Israel and J. M. M. Smits, The DIRDIF 94 program system, Technical Report of the Crystallography Laboratory, University of Nijmegen, 1994.
13 SHELXS 86, G. M. Sheldrick, in *Crystallographic Computing 3*, eds. G. M. Sheldrick, C. Kruger and R. Goddard, Oxford University Press, 1985, pp. 175–189.
14 DIFABS, N. Walker and D. Stuart, *Acta Crystallogr., Sect. A*, 1983, **39**, 158.
15 TEXSAN, Crystal Structure Analysis Package, Molecular Structure Corporation, Houston, TX, 1995.
16 H. Hou, B. Liang, X. Xin, K. Yu, P. Ge, W. Ji and S. Shi, *J. Chem. Soc., Faraday Trans.*, 1996, **92**, 2343.
17 J. M. Charnock, S. Bristow, J. R. Nicholson, C. D. Garner and W. Clegg, *J. Chem. Soc., Dalton Trans.*, 1987, 303.
18 A. Müller, H. Bogge and U. Schimanski, *Inorg. Chim. Acta*, 1980, **45**, L249.
19 A. Müller, H. Bogge and U. Schimanski, *Inorg. Chim. Acta*, 1983, **69**, 5 and refs. therein.
20 S. W. Du, N. Y. Zhu, P. C. Chen, X. T. Wu and J. X. Lu, *J. Chem. Soc., Dalton Trans.*, 1992, 339.
21 S. W. Du, N. Y. Zhu, P. C. Chen, X. T. Wu and J. X. Lu, *Polyhedron*, 1992, **11**, 109.
22 J. C. Huffman, R. S. Roth and A. R. Siedle, *J. Am. Chem. Soc.*, 1976, **98**, 1310.
23 S. Guha, C. C. Frazier, P. L. Porter, K. Kang and S. E. Finberg, *Opt. Lett.*, 1989, **14,** 952.
24 W. J. Blau, H. J. Byrne, D. J. Cardin and A. P. Davey, *J. Mater. Chem.*, 1991, **1**, 245.
25 J. S. Shirk, J. R. Lindle, F. J. Bartoli, Z. H. Kafafi and A. W. Snow, in *Materials for Nonlinear Optics*, eds. S. R. Marder, J. E. Sohn and G. D. Stucky, American Chemical Society, Washington, 1992, p. 626.
26 Y. Wang and L. T. Cheng, *J. Phys. Chem.*, 1992, **96**, 1530.
27 M. Sheik-Bahae, D. C. Hutching, D. J. Hagan and E. W. Van Stryland, *Phys. Rev. Lett.*, 1991, **65**, 96; R. DeSalvo, A. A. Said, D. J. Hagan, E. W. Van Stryland and M. Sheik-Bahae, *IEEE J. Quantum Electron.*, 1996, **32**, 1324.

Received 4*th December* 1996; *Paper* 6/08190H